Me₃SiC≡C–CMe=CH₂ copper(I) β-diketonates: Synthesis, solid state structure, and low-temperature chemical vapour deposition

Y. Shen [a], T. Rüffer [a], S.E. Schulz [b], T. Gessner [b], L. Wittenbecher [c], H.-J. Sterzel [d], H. Lang [a,*]

[a] *Technische Universität Chemnitz, Fakultät für Naturwissenschaften, Institut für Chemie, Lehrstuhl Anorganische Chemie, Straße der Nationen 62, 09111 Chemnitz, Germany*
[b] *Technische Universität Chemnitz, Fakultät für Elektrotechnik und Informationstechnik, Lehrstuhl für Mikrotechnologie, Zentrum für Mikrotechnologien, Reichenhainer Straße 70, 09126 Chemnitz, Germany*
[c] *BASF Aktiengesellschaft, GC/Z-M 311, 67056 Ludwigshafen, Germany*
[d] *BASF Aktiengesellschaft, ZAR/A-M 311, 67056 Ludwigshafen, Germany*

Abstract

The ene-yne copper(I) β-diketonates [(η²-TMSMB)Cu(β-diketonate)] (β-diketonate = *ac*etyl*ac*etonate/acac, **5**; = 1,3-*d*i-tert-*b*utyl*ac*etonate/dbac, **6**; = 1,1,1,5,5,5-*h*exa*f*luoroacetyl*ac*etonate/hfac, **7**; TMSMB = 4-*T*ri*M*ethyl*S*ilyl-2-*M*ethyl-*B*ut-1-ene-3-yne, Me₃SiC≡C–CMe=CH₂) are accessible by the reaction of [(η²-TMSMB)Cu(μ-Cl)]₂ (**3**) with [Na(β-diketonate)] (β-diketonate = acac, **4a**; = dbac, **4b**; = hfac, **4c**) in a 1:2 molar ratio. Complexes **6** and **7** are also formed, when Cu₂O (**8**) is reacted with H-hfac (**9a**) or H-dbac (**9b**), respectively.

The solid state structure of **7** is reported. The copper(I) ion possesses a planar environment caused by the η²-coordinated TMSMB ligand and the chelate-bound hfac group, while the CMe=CH₂ entity stays free.

The thermal properties of **5**–**7** were determined by applying *T*hermo*G*ravimetry (TG) and *D*ifferential *S*canning *C*alorimetry (DSC). All complexes decompose in a two-step process beginning at ca. 85 °C. Elimination of TMSMB produces [Cu(β-diketonate)] which disproportionates to give [Cu(β-diketonate)₂] and elemental copper.

Preliminary hot-wall *C*hemical *V*apour *D*eposition experiments (CVD) were carried out with **7**. Copper films were deposited onto TiN-coated oxidised silicon wafers at a precursor vaporisation temperature of 50 °C and a deposition temperature of 145 °C. The films were characterised by SEM and EDX.
© 2005 Elsevier B.V. All rights reserved.

Keywords: Copper(I); β-Diketonate; Ene-yne; CVD; SEM; EDX; X-ray

1. Introduction

The *C*hemical *V*apour *D*eposition (CVD) of pure copper films from Lewis-base-stabilised copper(I) complexes is substantial, since this technique is considered as alternative possibility for interconnect metallisation in future generations of sub-micron integrated circuits [1–3], which is attributed, for example, to the low resistivity and superior electro-migration resistance of copper [4–8]. Copper precursors should be volatile, preferentially monomeric with low molecular weight, and should be easy to handle before and during the deposition experiments. Among them, [LₙCu(β-diketonate)] complexes (L = 2-electron donor; n = 1, 2) have recently attracted

---

attention as CVD precursors, since the O,O-chelate-bound β-diketonate and the corresponding Lewis-bases L can be straightforward varied to tailor the volatility and stability of such systems [1,2,9–12]. As Lewis-bases L, phosphines, phosphites [11–13], alkenes [14–18], dienes [10,19], or alkynes [2,20,21] can be used to obtain an assortment of precursors with variable properties. The thermal decomposition of [Cu(β-diketonate)] occurs at low temperatures, generally in the range between 150 and 250 °C to give elemental copper along with [Cu(β-diketonate)$_2$] [22].

Recently, [(η^2-VTMS)Cu(hfac)] (VTMS = _V_inyl_T_ri-_M_ethyl_S_ilane, hfac = 1,1,1,5,5,5-_h_exa_f_luoroacetyl_ac_etonate) was commercially introduced as efficient, but thermal labile CVD copper precursor [23]. Other compounds of the same family have demonstrated valuable results [7,24,25]. Within this family of copper(I) CVD precursors, the physical properties can easily be varied by structural modifications, i.e. substitution reactions. Changing, for example, the Lewis-base L in [L$_n$Cu(β-diketonate)] (n = 1, 2) can directly alter the physical state, the vapour pressure, the decomposition temperature, and the long-term stability of the respective precursors [1,10]. For example, [(η^2-alkyne)Cu(hfac)] can be used as CVD precursor, however, a less volatile compound is formed in the bubbler along with elemental copper [21]. This unstable complex was thought to be bimetallic in which the alkyne unit binds to two copper(I) ions [26]. The formation of such species may be avoided by introducing both, π-conjugated vinyl or acetylenic units, and electron-withdrawing groups such as OCH$_3$ or CF$_3$, respectively [27]. The best results so far could be obtained, when the alkyne unit is conjugated with a vinyl entity [28].

We here describe the synthesis and characterisation of three [(η^2-alkyne-ene)Cu(β-diketonate)] species based on the 4-_T_ri_M_ethyl_S_ilyl-2-_M_ethyl-_B_ut-1-ene-3-yne (TMSMB) ligand. The use of one sample as CVD precursor for the deposition of copper onto oxidised silicon wafers covered with a CVD TiN film as a barrier is reported as well.

2. Results and discussion

2.1. Synthesis

The TMSMB-copper(I) β-diketonates **5–7** (TMSMB = 4-_T_ri_M_ethyl_S_ilyl-2-_M_ethyl-_B_ut-1-ene-3-yne, Me$_3$SiC≡C–CMe=CH$_2$) (Table 1) can be synthesised by treatment of [(η^2-TMSMB)Cu(μ-Cl)]$_2$ (**3**), which itself is accessible by the reaction of [CuCl] (**1**) with stoichiometric amounts of TMSMB (**2**) in dichloromethane solutions, with [Na(O$_2$C$_3$HR$_2$)] (**4a**, R = CH$_3$, _ac_etyl_ac_etonate, acac; **4b**, R = ^{t}Bu, 1,3-_di_-tert-_b_utyl_ac_etonate, dbac; **4c**, R = CF$_3$, 1,1,1,5,5,5-_h_exa_f_luoroacetyl_ac_etonate, hfac) in the ratio of 1:2 in diethyl ether at −30 °C (Scheme

Table 1
Synthesis of **5–7** by the reaction of **3** with **4**

Compound	R	β-Diketonate	Yield[a] (%)
5	Me	acac[b]	87
6	^{t}Bu	dbac[c]	84
7	CF$_3$	hfac[d]	79

[a] Based on **3**.
[b] _ac_etyl_ac_etonate.
[c] 1,3-_di_-tert-_b_utyl_ac_etonate.
[d] 1,1,1,5,5,5-_h_exa_f_luoroacetyl_ac_etonate.

1, Table 1). Complexes **6** and **7** can additionally be prepared by the reaction of H-hfac (**9a**) and H-dbac (**9b**) with Cu$_2$O (**8**) in presence of TMSMB (**2**) (Scheme 1).

After appropriate work-up, mononuclear **5–7** can be isolated in high yield (Table 1) as pale green (**5**), yellow (**6**) or off-white (**7**) materials of which **5** and **6** are liquids, while **7** melts at 32 °C. Complexes **5–7** are soluble in most common organic solvents, such as _n_-pentane, toluene, chloroform and diethyl ether. They are stable under inert gas atmosphere for months at −30 °C. On exposure to air they gradually decompose during days to give red solids which are not anymore soluble in common organic solvents.

2.2. Characterisation

Complexes **5–7** give satisfactory elemental analyses confirming the composition (TMSMB)Cu(β-diketonate). In addition, FT-IR, ^{1}H-, ^{13}C{^{1}H}- and ^{29}Si{^{1}H}-NMR spectroscopic studies were carried out. The solid state structure of **7** was established by X-ray structure determination.

For **5–7** one distinctive $v_{C≡C}$ vibration is found at 1930 (**5**), 1931 (**6**) or 1964 (**7**) cm^{-1} in the IR spectra. These absorptions are shifted to lower values, when compared with free _non_-coordinated TMSMB (2172 cm^{-1}) [28–30]. The magnitude of this change is related with the bond order and the nuclearity of the complex and is influenced by R of the O$_2$C$_3$HR$_2$ units. For **5–7** relatively small $\Delta v_{C≡C}$ values (**5**: 242, **6**: 241, **7**: 208 cm^{-1}) are obtained showing that in **7** somewhat weaker copper–carbon$_{alkyne}$ bonds are present as in **5** and **6**. These data correspond to other [(hfac)Cu(β-diketonate)] complexes and are in agreement with $\Delta v_{C≡C}$ characteristic for [(MHY)Cu(β-diketonate)] (MHY = 2-_M_ethyl-1-_H_exen-3-_Y_ne) [27]. Furthermore, two typical v_a(CO) and v_s(CO) absorptions are found between 1520 and 1660 cm^{-1}, whereby v_a corresponds to the asymmetric and v_s to the symmetric stretching vibration [27,31–34]. Δv_{CO} ($\Delta v_{CO} = v_a − v_s$) smaller than 70 cm^{-1} points to symmetrical, while larger values are typical for a asymmetrical bonding mode of the β-diketonates [32]. For **5–7** Δv_{CO} resembles to 67 (**5**, **7**) and 34 cm^{-1} (**6**) indicating that the β-diketonates are symmetrical O,O-chelate-bound
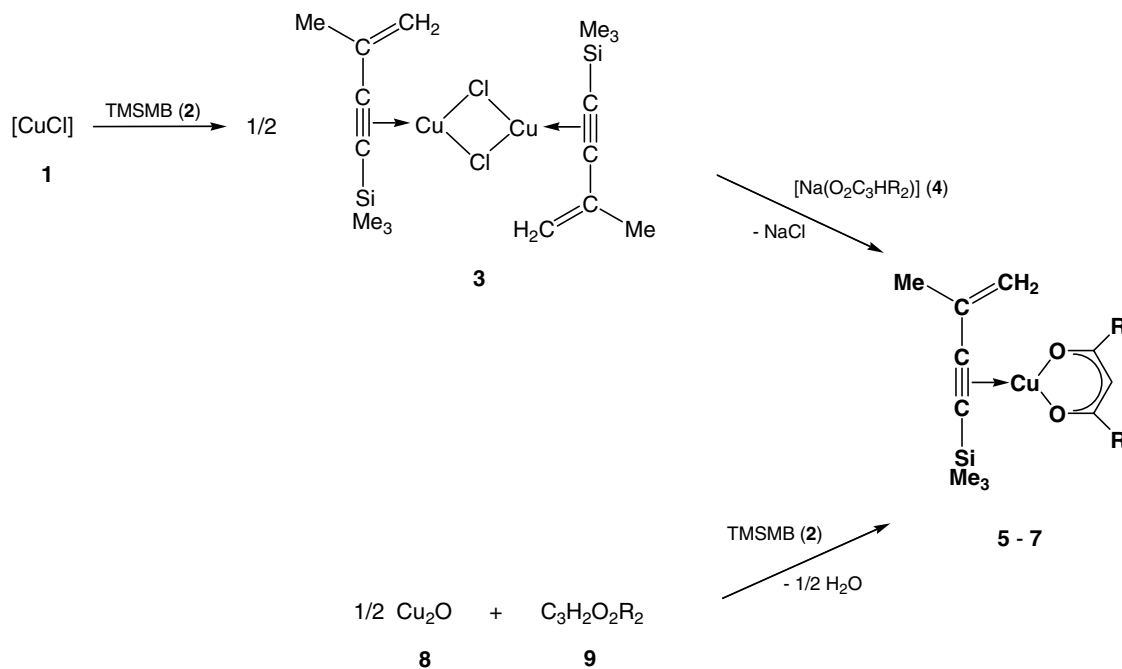
Scheme 1. Synthesis of **5**–**7** (Table 1).

to copper(I). This structural motif is also favoured in the solid-state as it could be confirmed by single X-ray structure analysis (Fig. 1). When one takes the highest frequency in the above mentioned region as an estimate of the strength of the donor–acceptor interaction between the β-diketonates and copper, than the strongest carbon–oxygen bonds/weakest copper–oxygen interactions are found for **7** [36].

The ^{1}H NMR spectra of **5**–**7** are consistent with the 1:1 TMSMB-copper(β-diketonate) stoichiometry. The methine group gives rise to a distinct resonance signal at 5.75 (**5**), 5.72 (**6**) or 6.13 ppm (**7**) which is typical for β-diketonates. The resonance signals for the TMSMB ene unit are somewhat shifted to lower field

(**5**: 5.37, 5.31; **6**: 5.55, 5.30; **7**: 5.81, 5.22 ppm), when compared with free TMSMB (**2**: 5.35, 5.25 ppm) [32]. This is attributed to the η^2-coordination of the carbon–carbon triple bond to copper(I). Although, the Me$_3$Si resonance signal (**5**: 0.31, **6**: 0.26, **7**: 0.32 ppm) is somewhat shifted to lower field (i.e. free TMSMB: 0.20 ppm) [29].

The ^{13}C{^{1}H} NMR spectra of **5**–**7** show that the TMSMB ligand only binds by the carbon–carbon triple bond to copper. This is in agreement with the observation made in the IR spectra of **5**–**7** (vide supra) and is typical for other ene-yne species, i.e. [(MHY)Cu(β-diketonate)] [27].

The C$_\alpha$ and C$_\beta$ TMSMB carbons (Me$_3$SiC$_\alpha$≡C$_\beta$) are low-field shifted (with exception of C$_\alpha$ of **7**) (for comparison, free TMSMB: C$_\alpha$ = 93.3, C$_\beta$ = 106.8; **5**: C$_\alpha$ = 99.9, C$_\beta$ = 113.6; **6**: C$_\alpha$ = 94.2, C$_\beta$ = 110.5; **7**: C$_\alpha$ = 92.9, C$_\beta$ = 112.9 ppm) confirming the η^2-coordination of TMSMB to copper(I) [35]. In contrast, the H$_2$C=CMe carbon atoms appear at almost the same chemical shift as in **2** indicating that there is no interaction of the ene unit with the group-11 metal ion (TMSMB: 123.2, 127.3 ppm; **5**: 123.4, 130.0 ppm; **6**: 123.2, 127.7 ppm; **7**: 124.7, 127.1 ppm). The CH fragment of the β-diketonates gives rise to one very characteristic resonance signal at 94.9 (**5**), 89.9 (**6**) or 89.6 ppm (**7**). The CO carbons are found between 178 and 202 ppm as it is expected for this type of building blocks [27]. It is obvious that the CO resonance signal for **7** (178.3 ppm) is significantly high field-shifted, when compared with **5** (190.6 ppm) and **6** (201.7 ppm). This trend is also found for [(MHY)Cu(acac)] (190.3 ppm) and [(MHY)Cu(hfac)]
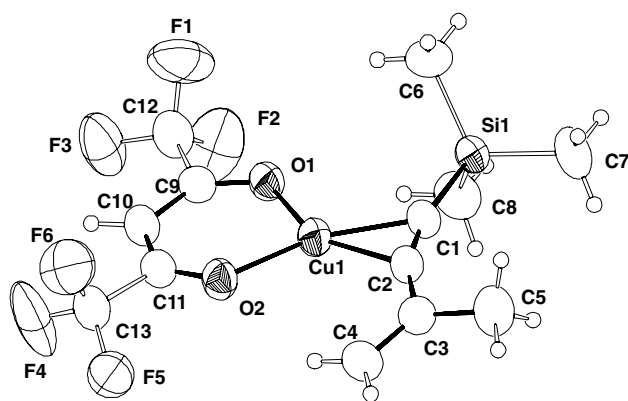

Fig. 1. XP PLOT (drawn at 50% probability level) of **7** with the adopted atom numbering scheme. Selected bond lengths [Å] and angles [°] are given in Table 2.

(178.4 ppm) and is attributed to the electronegative CF_3 groups [27].

In the $^{29}Si\{^1H\}$ NMR spectra of **5**–**7** a resonance signal is observed at −21.9 (**5**, **6**) or −10.2 ppm (**7**) for the Me_3Si group. The silicon atoms follow the order of deshielding (hfac < dbac, acac).

2.3. X-ray structure analysis

Single crystals of **7** could be grown from a saturated *n*-hexane/diethyl ether solution containing **7** at −30 °C. The molecular structure of **7** is shown in Fig. 1. Selected bond lengths [Å] and angles [°] are given in Table 2 and important crystal data and collection and refinement parameter are summarised in Table 5 (Section 3).

Complex **7** crystallises in the triclinic space group $P\bar{1}$. **7** contains a tri-coordinated copper(I) ion in a planar environment, caused by the two chelate-bound O(1) and O(2) hfac oxygen atoms and the η^2-coordinated TMSMB ligand (C(1), C(2)) (Fig. 1). This structural motif is typical for such species and is also found in [(η^2-MeC≡CMe)Cu(hfac)] [2], [(η^2-BTMSA)Cu(hfac)] (BTMSA = *B*is(*T*ri*M*ethyl*S*ilyl)*A*cetylene) [24] or [(η^2-MHY)Cu(hfac)] (MHY = 2-*M*ethyl-1-*H*exene-3-*Y*ne) [27].

The molecule scaffold with Cu(1), O(1), O(2), C(1)–C(3) and C(9)–C(11) is planar (max. deviation 0.09(2) Å, Si(1)) which best can be explained by the conjugated hfac and $Me_3SiC≡C–CMe=CH_2$ units (Table 3). The distortion of the C(2)–C(5) ene-yne plane (max. deviation 0.003(2) Å, C(3)) to the latter plane resembles to 11.7(2)° (Table 3).

The copper-alkyne bond distances in **7** are with 1.967(3) (Cu(1)–C(1)) and 1.973(3) Å (Cu(2)–C(2)) (Table 2) almost as long as those ones found in [(η^2-MHY)-

Table 2
Selected bond lengths (Å) and angles (°) for **7**[a]

Bond lengths

Cu(1)–O(1)	1.973(2)	C(3)–C(4)	1.329(4)
Cu(1)–O(2)	1.960(2)	C(3)–C(5)	1.512(4)
Cu(1)–C(1)	1.967(3)	C(9)–C(10)	1.403(4)
Si(1)–C(1)	1.871(3)	C(10)–C(11)	1.390(4)
Cu(1)–C(2)	1.973(3)	O(1)–C(9)	1.257(3)
C(2)–C(3)	1.455(4)	O(2)–C(11)	1.244(4)
Cu(1)–C(3)/C(4)[b]	3.221(4)	C(1)–C(2)	1.237(4)

Bond angles

O(1)–Cu(1)–O(2)	94.56(10)	Cu(1)–O(2)–C(11)	122.45(18)
O(1)–Cu(1)–C(1)	112.25(11)	C(1)–Cu(1)–C(2)	36.59(11)
O(1)–Cu(1)–C(2)	148.81(9)	O(1)–C(9)–C(10)	128.2(3)
C(1)–Cu(1)–O(2)	153.04(10)	O(2)–C(11)–C(10)	129.6(2)
C(2)–Cu(1)–O(2)	116.62(11)	C(2)–C(3)–C(4)	121.8(3)
Cu(1)–C(1)–C(2)	71.96(16)	C(1)–C(2)–C(3)	158.5(3)
Cu(1)–C(2)–C(1)	71.45(18)	C(2)–C(1)–Si(1)	166.5(2)
Cu(1)–O(1)–C(9)	122.61(17)	C(9)–C(10)–C(11)	122.5(3)

[a] The figures in parentheses represent the standard deviation in units of the last significant digits.
[b] Midpoint of the C(3)–C(4) carbon–carbon double bond.

Table 3
Deviations of defining atoms from the best-molecule-plane of **7**[a]

Atom	Deviation (Å)
Cu(1)	−0.017(8)
Si(1)	−0.09(2)
O(1)	0.008(2)
O(2)	−0.058(2)
C(1)	−0.044(2)
C(2)	0.003(2)
C(3)	0.05(2)
C(9)	0.019(2)
C(10)	0.030(2)
C(11)	−0.010(2)
r.m.s.d.	0.0323
C(2)	−0.0009(7)
C(3)	0.003(2)
C(4)	−0.0010(8)
C(5)	−0.0008(7)
r.m.s.d.	0.0016

[a] The figures in parentheses represent the standard deviation in units of the last significant digit.

Cu(hfac)] (1.94(1) and 1.95(1) Å) [26]. However, they are slightly shorter than the corresponding separations typical for the [(η^2-alkene)Cu(hfac)] family, e.g. 2.013(5) and 2.277(7) Å for [(η^2-1,5-COD)Cu(hfac)] (COD = *C*yclo*O*cta*D*iene) [36,37], or 2.011(3) and 2.029(3) Å for [(η^2-7-tert-butoxy-2,5-NBD)Cu(hfac)] (NBD = *N*or*B*orna*D*iene) [38]. This indicates a stronger interaction between the copper and the sp-hybridised carbon atoms, rather than that of η^2-coordinated alkenes. The C(1)–C(2) bond length with 1.237(4) Å is somewhat longer than the related separation in free 2-butyne (1.211 Å) which is typical for η^2-coordinated alkynes in transition metal chemistry [39]. The $H_2C=CMe$ entity is not interacting with Cu(1) (Cu(1)–C(3) 3.115, Cu(1)–C(4) 3.453 Å) (Fig. 1).

The copper–oxygen distances are 1.973(2) (Cu(1)–O(1)) and 1.960(2) Å (Cu(1)–O(2)) indicating a nearly symmetric binding of the β-diketonate to Cu(1). This structural behaviour is also found in solution (vide supra).

As expected, the alkyne unit deviates from linearity (*cis*-bending) upon ^{2}-coordination of TMSMB to copper(I) (C(1)–C(2)–C(3) 158.5(3), C(2)–C(1)–Si(1) 166.5(2)°) (Table 2 and Fig. 1).

2.4. TG and DSC studies, and chemical vapour deposition

*T*hermo*G*ravimetric studies (TG) were carried out to optimise the temperature at which **5**–**7** should best be maintained during the CVD experiment [40]. Complex **7** starts to decompose at 85 °C. The percentage of the residue at 400 °C is half as much as the theoretical percentage calculated for the formation of copper. Typical for **7** is a two-step decomposition in the temperature range of 85–250 °C. Between 85 and 170 °C the η^2-coordinated ene-yne ligand TMSMB is eliminated, which is evidenced

by the weight loss of 33.8%. In the second step (190–250 °C) the disproportionation of the in-situ generated [Cu(hfac)] species takes place to produce [Cu(hfac)$_2$] along with elemental copper. For **5** and **6** a similar behaviour is found which differs from the process displayed by their Cu(II) analogues (Section 3) [41].

Differential Scanning Calorimetry (DSC) shows the change of enthalpy during thermolysis. Complexes **5**–**7** possess two exothermic steps ($\Delta H = -46.49/-115.77$ (**5**); $-26.07/-32.48$ (**6**); $-150.75/-186.44$ J/g (**7**)). Complex **7** possesses an exothermic peak between 75 and 175 °C with the maximum at 137 °C, which corresponds to the dissociation of TMSMB from [(η^2-TMSMB)-Cu(hfac)]. The measured enthalpy for this process is -150.75 J/g. The disproportionation of in-situ formed [Cu(hfac)] to copper and [Cu(hfac)$_2$] takes place between 195 and 282 °C (peak maximum at 239 °C) with $\Delta H = -186.44$ J/g. This observation corresponds to other alkyne-stabilised copper(I) β-diketonates [12,21,27].

Based on the above mentioned data, **7** was selected to act as potential CVD precursor. In a typical deposition experiment, copper was deposited onto a TiN-coated oxidised silicon wafer at 145 °C by using a quartz tube horizontal hot-wall CVD reactor. The precursor temperature was maintained at 50 °C with a nitrogen flow of 14 sccm. The total pressure during the CVD experiment was maintained at 4.6×10^{-2} mbar with nitrogen as carrier gas. No reducing agent such as H$_2$ was used for the deposition experiment. The surface morphology and composition of the obtained copper films were examined with SEM and EDX.

The film deposited with **7** is copper coloured. In precursor flow direction, the colour appears more lightly related to smaller film thickness. In Fig. 2 a SEM image of this film is depicted.

The film is not completely closed and not homogeneous. Two kinds of copper grains are visible: small grains of about 180 nm size, the nucleation layer, which are evenly formed and are in the state of coalescence, and secondly, larger, irregular shaped grains of ca. 720 nm which are situated on the nucleation layer. The larger grains are the product of a homogeneous reaction in the gas phase. The deposition mechanism is changed from a heterogeneous reaction on the surface to a homogeneous reaction in the gas phase. There are several reasons for this change, which are not longer comprehensible, e.g. too low carrier gas flow or temperature variations.

EDX studies of the deposited copper films were carried out (Fig. 3, Table 4).

Apart from copper, also Si, Ti and O as substrate components could be determined. The reason for finding the latter elements is the small film thickness of about 200 nm. The larger grains were also characterised by using EDX. At those it was found that the percentage of copper is 98.78% (Si: 1.22%).

The deposition experiments with **7** show that this species is a very promising precursor for further detailed CVD studies.

3. Experimental

3.1. General procedure

All reactions were carried out under an atmosphere of purified nitrogen (O$_2$ traces: CuO catalyst, BASF AG, Ludwigshafen; H$_2$O: molecular sieve 4 Å) using standard Schlenk techniques. Diethyl ether was purified by distillation from sodium/benzophenone ketyl; *n*-pentane was purified by distillation from calcium hydride. Infrared spectra were recorded with a Perkin Elmer FT-IR 1000 spectrometer. ^{1}H, ^{13}C{^{1}H} and ^{29}Si{^{1}H} NMR spectra were recorded with a Bruker Avance 250 spectrometer. ^{1}H NMR spectra were recorded at 250.130 MHz, ^{13}C{^{1}H} NMR spectra at 62.895 MHz and ^{29}Si{^{1}H} NMR spectra at 49.662 MHz. Chemical shifts are reported in δ units (parts per million) downfield from tetramethylsilane with the solvent as the reference signal (^{1}H: C$_6$D$_6$, $\delta = 7.24$; ^{13}C{^{1}H}: C$_6$D$_6$, $\delta = 128.5$; ^{29}Si{^{1}H}: Me$_4$Si, $\delta = 0.0$). Melting points were determined using sealed nitrogen purged capillaries
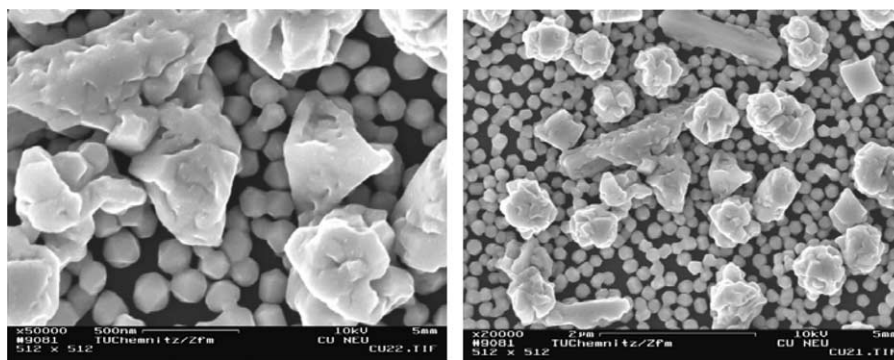

Fig. 2. SEM images showing the morphology of the copper film obtained from the chemical vapour deposition at 145 °C of **7**, deposited on a TiN-coated oxidised silicon wafer.
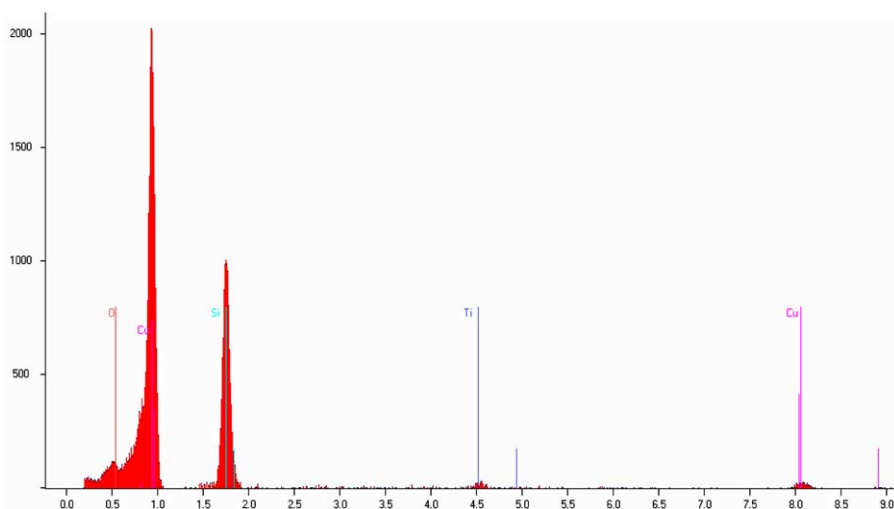
Fig. 3. EDX spectrum of the copper film obtained from **7** [T_s = 145 °C, P_{total} = 4.6 × 10^{-2} mbar; carry gas N$_2$; flow rate = 14 sccm].

on a Gallenkamp MFB 595 010 M melting point apparatus. Thermogravimetrical studies were carried out with the Perkin Elmer System Pyris TGA 6 and DSC studies with the Perkin Elmer System Pyris DSC 6. A constant heating rate of 8 K min^{-1} under nitrogen gas (1.0 cm^3/min) was used. SEM images were recorded with a SEM DSM 982 instrument, Gemini from LEO company. EDX analysis: EDX system EDWIN (Röntec company).

Microanalyses were performed by the Institute of Organic Chemistry, Chemnitz, Technical University and the Institute of Organic Chemistry, University of Heidelberg, Heidelberg.

For CVD experiments a quartz tube horizontal hot-wall reactor with 40 mm in diameter was used. Heating is achieved by a resistively heated tube oven (HORST company). The temperature is set by a temperature controller HT 520 (HORST company) and was calibrated with a thermocouple type GTH 1150 digital thermometer. The sample was placed in a glass container which is in direct contact with the quartz tube. Heating was performed with a heating-bend. Carrier gas flow was regulated using a MKS type 247 mass flow controller. The pressure control systems consist of an Edwards Active Gauge Controller, a cooling trap, and a turbo and a backing pump. The trap prevented the reactor effluents from entering the vacuum pump.

Table 4
EDX studies of the copper films obtained from **7** (T_s = 145 °C, P_{total} = 4.6 × 10^{-2} mbar; carrier gas N$_2$; flow rate = 14 sccm)

Element	Smaller particles (%)	Larger particles (%)
Cu	75.51	98.78
Si	13.08	1.22
O	8.68	–
Ti	2.72	–

Compounds **2**, [29] **3**, [15] and **4a**–**4c** [12] were prepared by published procedures. All other chemicals were purchased by commercial providers (Aldrich, VWR Chemicals) of highest grade and were used as received.

3.2. Synthesis of [(η²-TMSMB)Cu(acac)] (5)

To **3** (2.38 g, 5.0 mmol) dissolved in 40 mL of diethyl ether a suspension of Na(acac) (**4a**) (1.22 g, 10.0 mmol) in 40 mL of diethyl ether is added drop-wise during 10 min at −30 °C. After 4 h of stirring at this temperature all volatiles were removed in oil-pump vacuum. To the remaining liquid 100 mL of *n*-pentane are added. Filtration through a pad of Celite and evaporation of the solvent from the filtrate in oil-pump vacuum gives a pale green liquid in 2.55 g yield (8.65 mmol, 87% based on **3**).

Elemental analysis: Calc. for C$_{13}$H$_{21}$CuO$_2$Si (*300.94*): C, 51.89; H, 7.03. Found: C, 51.36; H, 6.79%. IR (NaCl): v[cm^{-1}] 3078 (w), 2959 (s), 2920 (s), 1930 (s) ($v_{C\equiv C}$), 1663 (w) ($v_{C=C}$), 1586 (vs) (CO, asym), 1519 (vs) (CO, sym), 1440 (vs), 1393 (vs), 1260 (s), 1194 (m), 1096 (m), 1016 (s), 978 (m), 922 (s), 863 (vs), 846 (vs), 764 (s), 701 (m), 637 (m), 578 (m), 536 (w), 472 (w). ^{1}H NMR (C$_6$D$_6$): δ 5.75 (s, 1H, CH/acac), 5.37 (s, 1H, =CH$_2$/TMSMB), 5.31 (s, 1H, =CH$_2$/TMSMB), 1.95 (s, 3H, CH$_3$/TMSMB), 2.03 (s, 6H, CH$_3$/acac), 0.31 (s, 9H, CH$_3$/SiMe$_3$, TMSMB). ^{13}C{^{1}H} NMR (C$_6$D$_6$): 190.6 (CO/acac), 130.0 (H$_2$C=C/TMSMB), 123.4 (H$_2$C=C/TMSMB), 113.6 (C≡C/TMSMB), 99.9 (C≡C/TMSMB), 94.9 (CH/acac), 28.3 (CH$_3$/acac), 24.0 (CH$_3$/TMSMB), 0.1 (CH$_3$/SiMe$_3$). ^{29}Si{^{1}H} NMR (C$_6$D$_6$): δ −21.9. TGA: T_{begin} = 80 °C, T_{end} = 170 °C, Δm = 44.15%; T_{begin} = 170 °C, T_{end} = 350 °C, Δm = 36.37%. DSC: Peak 1 = 171.3 °C (ΔH_1 = −46.49 J/g); Peak 2 = 190.1 °C (ΔH_2 = −115.77 J/g).

3.3. Synthesis of [(η^2-TMSMB)Cu(dbac)] (6)

Complex **6** can be synthesised as described for the preparation of **5** (Section 3.2). In this respect, 2.38 g (5.0 mmol) of **3** were reacted with 2.06 g (10.0 mmol) of **4b**. After appropriate work-up, complex **6** can be isolated as a pale yellow liquid in 3.24 g yield (8.4 mmol, 84% based on **3**).

Elemental analysis: Calc. for $C_{19}H_{33}CuO_2Si$ (*385.10*): C, 59.26; H, 8.64. Found: C, 58.69; H, 8.26%. IR (NaCl): ν[cm^{-1}] 3099 (w), 2958 (vs), 2903 (s), 2868 (s), 1931 (m) ($\nu_{C\equiv C}$), 1650 (m) ($\nu_{C=C}$), 1571 (vs) (CO, asym), 1537 (s) (CO, sym), 1457 (vs), 1432 (vs), 1409 (vs), 1359 (s), 1270 (m), 1248 (s), 1222 (s), 1184 (m), 1126 (m), 978 (m), 867 (s), 844 (s), 794 (m), 761 (m), 736 (m), 636 (m), 593 (m), 476 (s). ^{1}H NMR (C_6D_6): δ 5.72 (s, 1H, CH/dbac), 5.55 (s, 1H, =CH/TMSMB), 5.30 (s, 1H, =CH/TMSMB), 1.18 (s, 3H, CH_3/TMSMB), 1.05 (s, 18H, ^tBu/dbac), 0.26 (s, 9H, SiMe$_3$). ^{13}C{^{1}H} NMR (C_6D_6): δ 201.7 (CO/dbac), 127.7 ($H_2C=C$/TMSMB), 123.2 ($H_2C=C$/TMSMB) 110.5 ($C\equiv C$/TMSMB), 94.2 ($C\equiv C$/TMSMB), 89.9 (CH/dbac), 41.8 ($\underline{C}(CH_3)_3$/dbac), 29.0 (CH$_3$/^tBu, dbac), 23.9 (CH$_3$/TMSMB), 0.3 [SiMe$_3$/TMSMB], ^{29}Si{^{1}H} NMR (C_6D_6): δ −21.9. TGA: T_{begin} = 90 °C, T_{end} = 240 °C, Δm = 37.2%; T_{begin} = 240 °C, T_{end} = 500 °C, Δm = 45.6%. DSC: Peak 1 = 128 °C (ΔH_1 = −26.07 J/g); Peak 2 = 219 °C (ΔH_2 = −32.48 J/g).

3.4. Synthesis of [(η^2-TMSMB)Cu(hfac)] (7)

For the synthesis and work-up of **7** see Section 3.2. In this respect, 2.38 g (5.0 mmol) of **3** were reacted with 2.3 g (10.0 mmol) of **4c**. Complex **7** can be isolated as a off-white solid. Yield: 3.23 g (7.89 mmol, 79% based on **3**).

Mp: 32 °C. Elemental analysis: Calc. for $C_{13}H_{15}F_6CuO_2Si$ (*408.88*): C, 38.19; H, 3.70. Found: C, 37.85; H, 3.39%. IR (NaCl): ν[cm^{-1}] 2961 (w), 2926 (w), 2904 (w), 1964 (m) ($\nu_{C\equiv C}$), 1642 (s) ($\nu_{C=C}$), 1619 (m) (CO, asym), 1552 (m) (CO, sym), 1523 (m), 1477 (s), 1254 (s), 1200 (s), 1148 (vs), 1104 (m), 974 (w), 921 (m), 850 (s), 797 (m), 763 (m), 671 (m), 635 (w), 589 (w), 530 (w). ^{1}H NMR (C_6D_6): δ 6.13 (s, 1H, CH/hfac), 5.81 (s, 1H, =CH$_2$/TMSMB), 5.22 (s, 1H, =CH$_2$/TMSMB), 1.87 (s, 3H, CH$_3$/TMSMB), 0.32 (s, 9H, SiMe$_3$). ^{13}C{^{1}H} NMR (C_6D_6): δ 178.3 (CO/hfac, J_{C-F} = 38.7 Hz), 127.1 ($H_2C=C$/TMSMB), 124.7 ($H_2C=C$/TMSMB), 112.9 ($C\equiv C$/TMSMB), 92.9 ($C\equiv C$/TMSMB), 89.6 (CH/hfac), 118.5 (CF$_3$/hfac, J_{C-F} = 281.3 Hz), 23.6 (CH$_3$/TMSMB), −0.5 (CH$_3$/SiMe$_3$, TMSMB). ^{29}Si{^{1}H} NMR (C_6D_6): δ −10.2. TGA: T_{begin} = 85 °C, T_{end} = 170 °C, Δm = 33.8%; T_{begin} = 190 °C, T_{end} = 250 °C, Δm = 32.13%; T_{begin} = 275 °C, T_{end} = 350 °C, Δm = 14.54%. DSC: Peak 1 = 137 °C (ΔH_1 = −150.75 J/g); Peak 2 = 239.0 °C (ΔH_2 = − 186.44 J/g).

3.5. X-ray structure analysis of 7

Single crystals of **7** could be grown from a *n*-hexane/diethyl ether solution at −30 °C. One crystal was picked directly in the Schlenk flask under nitrogen flow and glued with resin (Araldit) on top of a glass needle. X-ray structure measurement was performed with a BRUKER SMART 1K CCD diffractometer. Crystal data, data collection and refinement details are given in Table 5.

The unit cell was determined with the program SMART [42]. For data integration and refinement of the unit cell the program SAINT [42] was used. The space group was determined using the program ABSEN [43]. All data were corrected for absorption using SADABS [44]. The structure was solved using direct methods (SHELX-97 [45]), refined using least square methods (SHELX-97 [45]). All *non*-hydrogen atoms were fully refined in their located positions, the hydrogen atoms were taken from the electron density difference map and refined freely.

Table 5
Crystal data and collection and refinement parameter for **7**

Formula	$C_{13}H_{15}F_6CuO_2Si$
Formula weight	408.88
Crystal colour	Greenish
Crystal dimensions (mm)	$0.90 \times 0.24 \times 0.10$
Crystal system	Triclinic
Space group	$P\bar{1}$
a (Å)	7.574(8)
b (Å)	10.825(11)
c (Å)	11.238(12)
α (°)	76.11(2)
β (°)	88.50(2)
γ (°)	86.17(2)
V (Å^3)	892.4(16)
Z value	2
D_{calc} (g cm^{-3})	1.522
Index ranges	$-10 \leqslant h \leqslant 10$, $-14 \leqslant k \leqslant 15$, $-7 \leqslant l \leqslant 16$
F (0 0 0)	412
μ (Mo Kα) (cm^{-1})	1.350
Radiation, Mo Kα	λ = 0.71073 Å
Temperature (K)	173(2)
$2\theta_{max}$	61.34
No. of reflections measured	7236
Independent reflections observed ($I \geqslant 2.00(\sigma(I))$)	4880
No. of refined parameters	212
R_1 ($I \geqslant 2\sigma(I)$)/all data[a]	0.0397/0.0736
WR_2 ($I \geqslant 2\sigma(I)$)/all data[b]	0.0991/0.1146
Goodness-of-fit (F^2)[c]	0.999
$\Delta\rho_{max}$ (e Å^{-3})	0.450
$\Delta\rho_{min}$ (e Å^{-3})	−0.313
Δ/σ_{max}	0.009

n = number of reflections, p = parameters used.

[a] $R_1 = \sum(|F_o - F_c|)/\sum|F_o|$; $wR_2 = \left[\sum(w(F_o^2 - F_c^2)^2)/\sum(wF_o^4)\right]^{1/2}$.

[b] $W = 1/[\sigma^2(F_o^2) + (0.0612P)^2]$, $P = (F_o^2 + 2F_c^2)/3$.

[c] $S = \left[\sum w(F_o^2 - F_c^2)^2\right]/(n-p)^{1/2}$.

4. Supplementary material

Crystallographic data for the structural analysis have been deposited with the Cambridge Crystallographic Data Centre, CCDC-No. 275398 for **7**. Copies of this information may be obtained free of charge from The Director, CCDC, 12 Union Road, Cambridge, CB2 1EZ UK (fax: +44-1223-336-033; e-mail: deposit@ccdc. cam.ac.uk or http://www.ccdc.cam.ac.uk).

Acknowledgement

References

[1] H.K. Shin, K.M. Chi, M.J. Hampden-Smith, T.T. Kodas, M.F. Paffett, J.D. Farr, Chem. Mater. 4 (1992) 788.
[2] T.H. Baum, C.E. Larson, Chem. Mater. 4 (1992) 365.
[3] D.B. Beach, F.K. LeGoues, C.K. Hu, Chem. Mater. 2 (1990) 216.
[4] J. Li, R. Blewer, J.W. Mayer, MRS Bull. 18 (1993) 18.
[5] T.L. Alford, J. Li, J.W. Mayer, S.Q. Wang, Thin solid Films 262, VII (1995).
[6] P.L. Pai, C.H. Ting, IEEE Electron Device Lett. 10 (1989) 423.
[7] T.T. Kodas, M.J. Hampden-Smith, The Chemistry of Metal CVD, VCH, Weinheim, 1994.
[8] A. Jain, K.M. Chi, H.K. Chi, J. Farkas, T.T. Kodas, M.J. Hampden-Smith, Semicond. Int. 16 (1993) 128.
[9] J.A.T. Norman, B.A. Muratore, P.N. Dyer, D.A. Roberts, A.K. Hochberg, June 11–12, 1991 VMIC Conference, IEEE, P 123.
[10] S.K. Reynolds, C.J. Smart, E.F. Baran, T.H. Baum, C.E. Larson, P.J. Brock, J. Appl. Phys. Lett. 59 (1991) 2332.
[11] A. Jain, K.M. Chi, M.J. Hampden-Smith, T.T. Kodas, M.F. Paffett, J.D. Farr, Chem. Mater. 3 (1991) 995.
[12] K.M. Chi, T.S. Corbitt, M.J. Hampden-Smith, T.T. Kodas, E.N. Deusler, J. Organomet. Chem. 449 (1993) 181.
[13] H.K. Shin, M.J. Hampden-Smith, T.T. Kodas, E.N. Duesler, Polyhedron 10 (1991) 645.
[14] C.H. June, Y.T. Kim, J.T. Baek, H.J. Yoon, D.R. Kim, J. Vac. Sci. Technol. A 14 (6) (1996) 3214.
[15] M.Y. Park, J.H. Son, S.W. Rhee, Electrochem. Solid-state Lett. 1 (1998) 32.
[16] J.H. Son, M.Y. Park, S.W. Rhee, Thin Solid Films 335 (1998) 229.
[17] Y.J. Senzaki, Electrochem. Soc. 145 (1998) 362.
[18] S.W. Rhee, S.W. Kang, S.H. Han, Electrochem. Solid-state Lett. 3 (2000) 135.
[19] P. Doppelt, T.H. Baum, L. Ricard, Inorg. Chem. 35 (1996) 1286.
[20] T.H. Baum, C.E. Larson, J. Electrochem. Soc. 140 (1993) 154.
[21] P. Doppelt, T.H. Baum, J. Organomet. Chem. 517 (1996) 53.
[22] G.A. Pehrsen, J.E. Parmehr, C.A. Apblett, M.F. Gonzales, P.M. Smith, T.R. Omslead, T.R. Norman, J. Electrochem. Soc. 142 (1995) 939.
[23] J.A.T. Norman, B.A. Muratore, P.N. Dyer, D.A. Roberts, A.K. Hochberg, J. Phys. IV (Paris) (1991) C2–C271.
[24] P. Doppelt, T.H. Baum, MRS Bull. XIX (8) (1994) 41.
[25] P. Doppelt, Coord. Chem. Rev. 180 (1998) 1783.
[26] T.Y. Chen, J. Vaissermann, P. Doppelt, Inorg. Chem. 40 (2001) 6167.
[27] T.Y. Chen, J. Vaissermann, R. Ruiz, J.P. Senateur, P. Doppelt, Chem. Mater. 13 (2001) 3393.
[28] R.U. Kirss, D. Gordon, P.S. Kirlin, Mater. Res. Soc. Symp. Proc. 282 (1993) 275.
[29] C.S. Rouvier, S. Ldfrere, M. Santelli, Tetrahedron Lett. 40 (1999) 5491.
[30] Y.J. Chen, H.D. Kaesz, H. Thridandam, R.F. Hicks, Appl. Phys. Lett. 53 (1988) 1591.
[31] Y.Z. Shen, M. Leschke, S.E. Schulz, T. Gessner, H. Lang, Chinese J. Inorg. Chem. 20 (2004) 1257.
[32] J.K. O'Loane, M.K. Wilson, J. Chem. Phys. 23 (1995) 1313.
[33] W.A. Anderson, A.J. Carty, G.J. Palenik;, G. Schreiber, Can. J. Chem. 49 (1971) 761.
[34] T.H. Baum, C.E. Larson, G.J. May, J. Organomet. Chem. 425 (1992) 189.
[35] M.E. Gross, V.M. Donnelly, in: V.S. Rana, R.V. Joshi (Eds.), Adv. Matallization for ULSI Applications, Materials Research Society, Pittsburgh, 1991, p. 355.
[36] K.M. Chi, H.K. Shin, M.J. Hampden-Smith, E.N. Duesler, Polyhedron 10 (1991) 2293.
[37] R. Kumar, F.R. Fronczek, A.W. Maverick, W.G. Lai, G.L. Griffin, Chem. Mater. 4 (1992) 577.
[38] K.M. Chi, H.C. Hou, P.T. Huang, Organometallics 14 (1995) 2641.
[39] E. Pignataro, B. Post, Acta Crystallogr. 8 (1955) 672.
[40] K.J. Eisentraut, R.E. Sievers, J. Inorg. Nucl. Chem. 29 (1976) 1931.
[41] N.S. Borgharkar, G.L. Griffin, J. Electrochem. Soc. 145 (1) (1998) 347.
[42] Bruker AXS Inc., Madison, WI, USA, 1998.
[43] P. McArdle, J. Appl. Cryst. 29 (1996) 306.
[44] G.M. Sheldrick, SADABS V 2.01, Program for Empirical Absorption Correction of Area Detector Data, University of Göttingen, Germany, 2000.
[45] G.M. Sheldrick, SHELX-97, Programs for Crystal Structure Analysis (Release 97-2), University of Göttingen, Germany, 1997.